SCIENTIFIC REPORTS

OPEN

SUBJECT AREAS:
PHYSICAL CHEMISTRY
THEORETICAL CHEMISTRY

Received
17 June 2014

Accepted
17 September 2014

Published
13 October 2014

Correspondence and requests for materials should be addressed to G.Y. (theobiochem@gmail.com)

Zwitterionic versus canonical amino acids over the various defects in zeolites: A two-layer ONIOM calculation

Gang Yang & Lijun Zhou

College of Resources and Environment & Chongqing Key Laboratory of Soil Multi-scale Interfacial Process, Southwest University, 400715, Chongqing, China.

Defects are often considered as the active sites for chemical reactions. Here a variety of defects in zeolites are used to stabilize zwitterionic glycine that is not self-stable in gas phase; in addition, effects of acidic strengths and zeolite channels on zwitterionic stabilization are demonstrated. Glycine zwitterions can be stabilized by all these defects and energetically prefer to canonical structures over Al and Ga Lewis acidic sites rather than Ti Lewis acidic site, silanol and titanol hydroxyls. For titanol (Ti-OH), glycine interacts with framework Ti and hydroxyl sites competitively, and the former with Lewis acidity predominates. The transformations from canonical to zwitterionic glycine are obviously more facile over Al and Ga Lewis acidic sites than over Ti Lewis acidic site, titanol and silanol hydroxyls. Charge transfers that generally increase with adsorption energies are found to largely decide the zwitterionic stabilization effects. Zeolite channels play a significant role during the stabilization process. In absence of zeolite channels, canonical structures predominate for all defects; glycine zwitterions remain stable over Al and Ga Lewis acidic sites and only with synergy of H-bonding interactions can exist over Ti Lewis acidic site, while automatically transform to canonical structures over silanol and titanol hydroxyls.

Zeolites are a family of crystalline microporous and mesoporous materials, and framework substitution of Si^{4+} by Al^{3+}, Ga^{3+}, Ti^{4+}, Sn^{4+} or other cations endows zeolites with variable adsorption and catalytic performances[1–3]. Nonetheless, the stability of zeolites will be reduced by framework substitution resulting in the formation of defect sites[4–7]. It has been claimed that defects in zeolites are active sites for a number of chemical reactions such as glucose isomerization to fructose, one of the key steps in biomass conversions[7–12].

When treated at high temperatures (inert atmosphere or steaming), three-coordinated Al sites that are kept in the framework of zeolites were detected, and increase of temperatures facilitated the conversion to such Al species[13,14]. Three-coordinated framework metal cations show Lewis acidity and are good catalysts for a number of chemical reactions; for instance, Fe Lewis acidic site shows superior catalysis for the direct benzene hydroxylation than ion-exchanged Fe sites[15–17]. Under physiological conditions, a variety of biomolecules exist as zwitterions. Zwitterionic structures exhibit strong electric fields around and this is the driving force to decide their properties and functions. Amino acid zwitterions in gas phase are not geometrically stable and have been stabilized by a lot of attempts, such as protonation[18,19], hydration[20–23], metalation[24–28], electron attachment[29,30] and anion addition[31–34]. Recently, interactions of amino acids with zeolites that are regarded as "solid solvents[35,36]" have emerged as a research focus[37–47], while no report has been given in regard to three-coordinated framework Al species. Can zwitterionic glycine be stabilized by such Al site with Lewis acidity? What about the relative stability vs. canonical conformers and the activation barrier of intramolecular proton transfer reactions? Are the zwitterionic stabilization effects correlated with the Lewis acidic strengths of framework three-coordinated metal cations (M = Al, Ga)?

All-silica zeolites are hydrophobic while defect silanol (Si-OH) is hydrophilic and thus can regulate the hydrophobic/hydrophilic property of silica zeolites. The previous studies focused on silica surfaces[37–41,43–45], and the results indicated that one silanol defect on the surface is not sufficient to stabilize zwitterionic glycine. What if the silanol defect situates within the channels of "solid-solvent" zeolites[35,36]? An analog was observed in TS-1 zeolite, as titanol (Ti-OH) that constitutes an important source of Lewis acidity[48]. The discovery of TS-1 zeolite has been recognized as a milestone in heterogeneous catalysis[3]. Can silanol and titanol defects within zeolite channels stabilize zwitterionic glycine and will they behave different during the zwitterionic stabilization and intramolecular proton transfer processes?

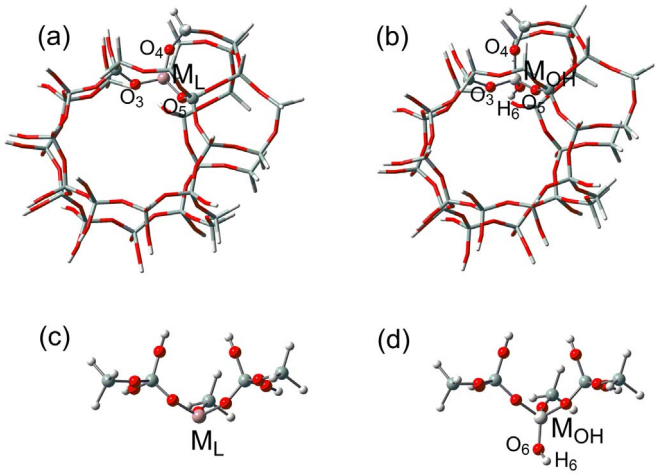

Figure 1 | 32-T and 6-T cluster models representing the local structures of MFI-type zeolites with (a, c) three-coordinated framework M Lewis acidic sites (M_L, M = Al, Ga) and (b, d) defect silanol/titanol (M_{OH}, M = Si, Ti).

In this work, the issues posed above were tackled by two-layer ONIOM calculations: (1) Stabilize zwitterionic and canonical glycine by three-coordinated framework Al and Ga sites and correlate the Lewis acidic strengths with zwitterionic stabilization effects; (2) Perform calculations as (1) for silanol and titanol defects and demonstrate their stabilization effects for zwitterionic glycine; (3) Study the intramolecular proton transfer reactions between zwitterionic and canonical glycine over these defect sites. In addition, two relating issues will be explored: (4) Clarify the role of zeolite channels during the zwitterionic stabilization by comparing the calculated results of 6-T and 32-T (default) cluster models (Figure 1); (5) It is known that framework Ti in zeolites displays Lewis acidity, and glycine should interact competitively over the Ti and hydroxyl sites of defect titanol (Ti-OH). Such competitive interaction processes will be demonstrated as well.

Results

The three-coordinated Al sites that remain in the framework of zeolites show Lewis acidity[14,17] and are expected to interact with the carboxylic moiety of amino acids. This has been corroborated by the calculated results that Al forms direct bond with the carboxylic-O2 atom of glycine, see Figure 2. As indicated in Table 1, the N-H*/O1-H* distances in **Zw** (Figure 2a) and **Can** (Figure 2b) are equal to 1.026/2.399 and 1.602/1.048 Å, and the corresponding glycine conformers are zwitterionic and canonical, respectively. That is, the zwitterionic glycine, which is not self-stable in gas phase[29], represents an energy minimum when adsorbed on framework Al Lewis acidic site. Whether zwitterionic or canonical, glycine forms several

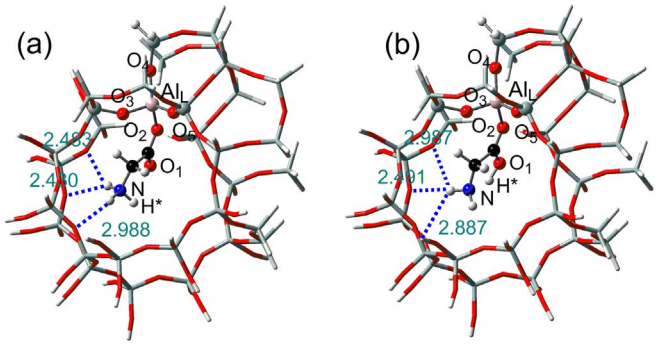

Figure 2 | Interactions of Al Lewis acidic site in ZSM-5 zeolite (32-T cluster models) with (a) zwitterionic and (b) canonical glycine. Selected distances are given in Å.

H-bonds with lattice-O atoms of zeolites, which resembles the situation in aqueous solutions and benefits the zwitterionic formation and stabilization[20–23]. The energy calculations indicate that the zwitterionic rather than canonical glycine is preferred by 5.1 kJ mol^{-1} (Table 1). However, in the case of H-form zeolite the canonical structure is obviously more stable[42], and so the formation of three-coordinated framework Al sites in zeolites substantially enhances the relative stability of zwitterionic vs. canonical glycine.

Like Al, trivalent Ga is often incorporated into the framework of zeolites[49]. The LUMO and LUMO + n (n = 1, 2, 3) of three-coordinated Al and Ga sites are shown in supplementary Figure S6 and indicate the presence of Lewis acidities for both species, which is supported by the strong adsorption of glycine. The adsorption energies of canonical glycine (ΔE_{ads}) on such Al and Ga species are calculated to be −190.0 and −157.6 kJ mol^{-1}, respectively. Accordingly, framework three-coordinated Al site has a higher Lewis acidity. As indicated in Figures 2, 3 and Table 1, glycine structures over Ga and Al Lewis acidic sites are rather close to each other. Although the Lewis acidic strengths differ greatly, three-coordinated Al and Ga sites have nearly the same stabilizing effects for zwitterionic glycine, and the energy differences (ΔE_{rel}) of zwitterionic vs. canonical glycine are equal to −3.8 and −5.1 kJ mol^{-1}, respectively.

Interactions of glycine with defect silanol (Si-OH) on silica surface have been extensively investigated[37–41,43–45], and here we focus on silanol within the channels of zeolites that behave like "solid solvents[35,36]". One silanol defect at the surface is not sufficient to stabilize glycine in the zwitterionic form[37], while the situation changes within zeolite channels. As shown in Figure 4, zwitterionic glycine has been stabilized as a stationary point by one silanol that situates within zeolite channels, mainly due to the co-existence of several strong H-bonds with lattice-O atoms. Four and five H-bonds are detected in **Zw1** (Figures 4a) and **Zw2** (Figure 4c), respectively. Note that H-bonds with distance below 3.0 Å have been counted, and more can be found if defined with 3.5 Å or larger distances.

Table 1 | Selected distances (r, Å), Mulliken charges (Q) and relative stability (ΔE_{rel}, kJ mol^{-1}) for zwitterionic vs. canonical glycine adsorbed over the framework Lewis acidic sites (M_L, M = Al, Ga) in ZSM-5 zeolites (32-T cluster models)[a, b]

	r(C1-O1)	r(C1-O2)	r(O1-H*)	r(N-H*)	r(M-O2)	Q_{Gly}	ΔE_{rel}
Can(Al_L)	1.291	1.258	1.048	1.602	1.875	0.277	−190.0 [c]
TS(Al_L)	1.275	1.265	1.167	1.362	1.863	0.291	7.7
Zw(Al_L)	1.230	1.300	2.399	1.026	1.828	0.336	−5.1
Can(Ga_L)	1.290	1.258	1.045	1.615	1.924	0.263	−157.6 [c]
TS(Ga_L)	1.274	1.265	1.164	1.369	1.913	0.276	8.4
Zw(Ga_L)	1.228	1.304	2.410	1.026	1.884	0.322	−3.8

[a]At the ONIOM(M06L/6-311++G**:B3LYP/6-31G*)//ONIOM(B3LYP/6-31+G**:B3LYP/3-21G) level;
[b]Structures with canonical glycine are used for energy benchmarks;
[c]Interaction energies between glycine and zeolite in these cases.

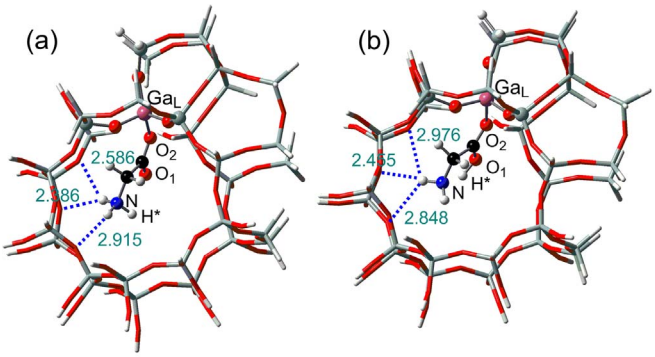

Figure 3 | Interactions of Ga Lewis acidic site in ZSM-5 zeolite (32-T cluster models) with (a) zwitterionic and (b) canonical glycine. Selected distances are given in Å.

Silanol (Si-OH) also forms H-bond with glycine, which is significantly stronger than those from lattice-O atoms as reflected from the short O6-H* distance (ca. 1.63 Å, Table 2). The stabilization effects of defect silanol are not so obvious as framework Al and Ga Lewis acidic sites, and zwitterionic glycine is no longer energy-preferred. The relative energies (ΔE_{rel}) of **Zw1** vs. **Can1** and **Zw2** vs. **Can2** are equal to 35.0 and 28.6 kJ mol^{-1}, respectively.

The acidity of defect silanol (Si-OH) in silica zeolites can be evaluated by proton affinity (PA),

$$\text{Zeo}-\text{Si}-\text{OH} \rightarrow \text{Zeo}-\text{Si}-\text{O}^- + \text{H}^+ \quad (1)$$

$$\text{PA} = E(\text{Zeo}-\text{Si}-\text{O}^-) - E(\text{Zeo}-\text{Si}-\text{OH}) \quad (2)$$

where E(Zeo-Si-OH) and E(Zeo-Si-O$^-$) refer to the energies of defect silanol and its deprotonated form, respectively.

The calculated PA for silanol defect equals 1497.9 kJ mol^{-1} and such a high value indicates its low acidity, consistent with the experimental observations[50]. In TS-1 zeolite, defect titanol (Ti-OH) is an important source of Lewis acidity[48], and here the stabilization effects of its hydroxyl is considered and compared with the results of silanol. The proton affinity (PA) for titanol is calculated in the same way and amounts to 1432.3 kJ mol^{-1}. Accordingly, framework Ti substitution improves the hydroxyl acidity although limited.

Interaction structures of titanol hydroxyl with glycine are shown in Figure 5, from where it can be found the H-bonds of glycine with lattice-O atoms are altered by Ti substitution. As compared to silanol, the H6-O2 H-bonds in titanol are reinforced (Tables 2 and 3), which is in line with the PA analyses; nonetheless, the acidity enhancement does not result in an observable increase of zwitterionic stability. Neither of the two zwitterions (**Zw1** and **Zw2**) is energy-preferred in the case of titanol hydroxyl and the relative energies of zwitterionic vs. canonical structures (ΔE_{rel}) are 35.3 and 25.4 kJ mol^{-1}, respectively. The adsorption energies (ΔE_{ads}) of canonical

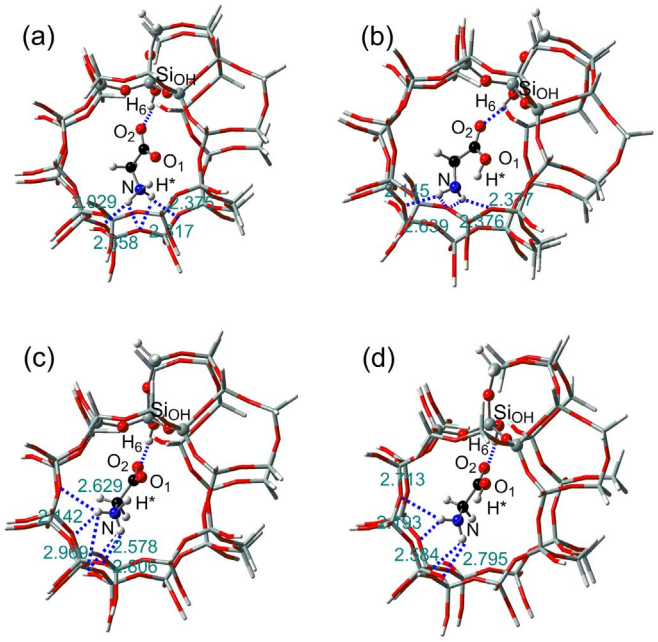

Figure 4 | Interactions of defect silanol (Si-OH) in Silicalite-1 (32-T cluster models) with (a, c) zwitterionic and (b, d) canonical glycine. Selected distances are given in Å.

glycine (**Can1** and **Can2**) are respectively calculated at −59.3 and −73.8 kJ mol^{-1} for titanol and −61.1 and −68.1 kJ mol^{-1} for silanol, in good agreement with the trend of zwitterionic stabilization effects. A more careful analysis of the correlation between relative stabilities and adsorption energies will be given latter.

The results above indicate that three-coordinated framework Al and Ga species show satisfactory stabilization effects to the zwitterionic glycine, and what about the four-coordinated framework Ti species that also displays Lewis acidity? As indicated in Figure 6, glycine can interact directly with Ti Lewis acidic site as NH_3 and H_2O reported previously[22,51,52], and the zwitterionic structure represents an energy minimum as in the cases of Al and Ga Lewis acidic sites. The Ti-O2 bonds in the zwitterionic and canonical structures are equal to 2.038 and 2.191 Å, respectively. However, the zwitterion is less stable than the canonical structure (ΔE_{rel} = 14.1 kJ mol^{-1}), and therefore Ti Lewis acidic site has inferior zwitterionic stabilization effects than Al and Ga Lewis acidic sites. In **Zw** (Figure 6a), the O6 atom of the titanol defect has a short distance with the carboxylic-O2 atom (2.696 Å), and this evidences strong repulsions although counteracted somewhat by H6-O2 H-bonding. Hence, for canonical glycine (Figure 6b), a smaller adsorption energy than Al and Ga Lewis acidic sties is expected for Ti Lewis acidic site and confirmed by the calculated results (ΔE_{ads} = −107.7 kJ mol^{-1}, Table 4). For

Table 2 | Selected distances (r, Å), Mulliken charges (Q) and relative stability (ΔE_{rel}, kJ mol^{-1}) for zwitterionic vs. canonical glycine adsorbed over the silanol group (Si$_{OH}$) in Silicalite-1 (32-T cluster models)[a, b]

	r(C1-O1)	r(C1-O2)	r(O1-H*)	r(N-H*)	r(H6-O2)	Q_{Gly}	ΔE_{rel}
Can1(Si$_{OH}$)	1.320	1.226	1.001	1.835	1.702	0.082	−61.1 [c]
TS1(Si$_{OH}$)	1.276	1.243	1.320	1.215	1.631	0.098	39.7
Zw1(Si$_{OH}$)	1.252	1.258	1.720	1.064	1.588	0.112	35.0
Can2(Si$_{OH}$)	1.324	1.226	1.006	1.772	1.781	0.088	−68.1 [c]
TS2(Si$_{OH}$)	1.280	1.243	1.334	1.199	1.671	0.113	33.0
Zw2(Si$_{OH}$)	1.263	1.253	1.588	1.087	1.627	0.126	28.6

[a]At the ONIOM(M06L/6-311++G**:B3LYP/6-31G*)//ONIOM(B3LYP/6-31+G**:B3LYP/3-21G) level;
[b]Structures with canonical glycine are used for energy benchmarks;
[c]Interaction energies between glycine and zeolite in these cases.

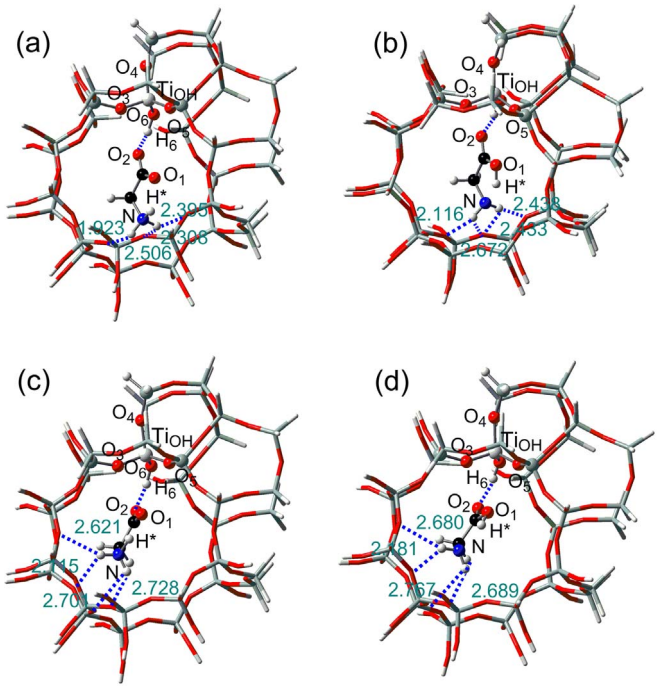

Figure 5 | Interactions of defect titanol (Ti-OH) in TS-1 zeolite (32-T cluster models) with (a, c) zwitterionic and (b, d) canonical glycine. Selected distances are given in Å.

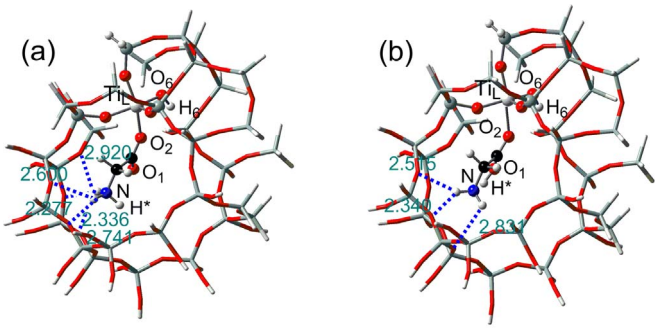

Figure 6 | Interactions of Ti Lewis acidic site (Ti_L) in TS-1 zeolite (32-T cluster models) with (a) zwitterionic and (b) canonical glycine. Selected distances are given in Å.

titanol (Ti-OH), Ti Lewis acidic site shows an enhancement of zwitterionic stabilization than the hydroxyl, see the ΔE_{rel} values in Tables 3 and 4; in addition, because of the formation of direct Ti-O2 bond, the adsorption of glycine on Ti Lewis acidic site is energetically preferential, and so this interaction mode predominates for glycine interactions with defect titanol (Ti-OH).

Discussion

Transition states (**TS**) for the transformation of canonical (**Can**) to zwitterionic (**Zw**) structures are displayed in supplementary Figures S7∼S9. As indicated in Tables 1∼4, for each intramolecular proton transfer reaction, the O1-H* distance is gradually enlarged from **Can** to **TS** and then to **Zw** whereas the N-H* distance changes in the opposite trend. Take Ti Lewis acidic site for example. The O1-H*/N-H* distances are respectively calculated to be 1.008/1.816, 1.228/1.298 and 2.718/1.024 Å in **Can**, **TS** and **Zw**, indicating the O1-H* bond rupture and N-H* bond formation during the intramolecular proton transfer process. Along with the proton transfers, the two carboxylic C-O distances become more close and approximately equivalent in the cases of defect hydroxyls (Tables 2 and 3), while in the cases of Al, Ga and Ti Lewis acidic sites, these two bonds are nearly equidistance in the transition states and apt to single/double in zwitterionic and canonical structures, which are mainly caused by the presence of M-O2 bonds (M = Al, Ga and Ti, Tables 1 and 4). The energy diagrams of the intramolecular proton transfer reactions over these defect sites are plotted in Figure 7, and the energy barriers increase as Al_L (7.7) < Ga_L (8.4) < Ti_L (24.5) < Ti_{OH2} (32.8) < Si_{OH2} (33.0) < Ti_{OH1} (38.6) < Si_{OH1} (39.7), with energy units of kJ mol^{-1}. It can be seen that the transformations from canonical to zwitterionic glycine are much more facile on Al and Ga Lewis acidic sites rather than on silanol/titanol hydroxyls and Ti Lewis acidic site.

An indicated in Figure 8, a good correlation can be established between zwitterionic stabilization effects and adsorption energies. The larger adsorption energy causes an increase of the relative stability of zwitterionic vs. canonical glycine and further results in the more facile proton transfer transformation characterized by a smaller energy barrier (Figure 7). Figure 9 shows that more charges will be transferred from zeolites to zwitterionic glycine when interacted more strongly, and more charge transfer is considered to be favourable for the stabilization of zwitterionic amino acids[28]. The only exception is titanol hydroxyl (Ti_{OH1}, see Figure 5), and overall, the adsorption energies (ΔE_{ads}) are closely associated with the amounts of charges transferred from zeolites to glycine (Q_{Gly}). Thus, it clearly demonstrates that charge transfers are the most significant factor to determine the zwitterionic stabilization effects. For each intramolecular proton transfer reaction, the charges on glycine increase along with the reaction coordinate; that is, $Q_{Zw} > Q_{TS} > Q_{Can}$, and zwitterionic structures always carry the most charges (Tables 1∼4).

As reflected from the numerous H-bonding interactions between glycine and lattice-O atoms, zeolite channels should play a significant role during the interactions of glycine and zeolites and this will be further demonstrated by density functional calculations with 6-T cluster models. As indicated in supplementary Tables S2∼S5 and Figure S1∼S5, in the absence of zeolite channels (6-T cluster models), a pronounced decrease of zwitterionic stability has been observed for all defects. The zwitterionic glycine over the hydroxyls

Table 3 | Selected distances (r, Å), Mulliken charges (Q) and relative stability (ΔE_{rel}, kJ mol^{-1}) for zwitterionic vs. canonical glycine adsorbed over the titanol group (Ti_{OH}) in TS-1 zeolite (32-T cluster models)[a, b]

	r(C1-O1)	r(C1-O2)	r(O1-H*)	r(N-H*)	r(H6-O2)	Q_{Gly}	ΔE_{rel}
Can1(Ti_{OH})	1.321	1.228	1.001	1.839	1.653	0.110	−59.3 [c]
TS1(Ti_{OH})	1.277	1.245	1.299	1.233	1.539	0.135	38.6
Zw1(T_{OH})	1.247	1.265	1.822	1.051	1.443	0.167	35.3
Can2(Ti_{OH})	1.328	1.226	1.006	1.775	1.767	0.114	−73.8 [c]
TS2(Ti_{OH})	1.283	1.244	1.309	1.218	1.609	0.143	32.8
Zw2(Ti_{OH})	1.261	1.256	1.652	1.073	1.560	0.165	25.4

[a]At the ONIOM(M06L/6-311++G**:B3LYP/6-31G*)//ONIOM(B3LYP/6-31+G**:B3LYP/3-21G) level;
[b]Structures with canonical glycine are used for energy benchmarks;
[c]Interaction energies between glycine and zeolite in these cases.

Table 4 | Selected distances (r, Å), Mulliken charges (Q) and relative stability (ΔE_{rel}, kJ mol^{-1}) for zwitterionic vs. canonical glycine adsorbed over the framework Ti Lewis acidic site (Ti_L) in TS-1 zeolite (32-T cluster models)[a, b]

	r(C1-O1)	r(C1-O2)	r(O1-H*)	r(N-H*)	r(Ti-O2)	Q_{Gly}	ΔE_{rel}
Can(Ti_L)	1.311	1.238	1.008	1.816	2.191	0.159	−107.7 [c]
TS(Ti_L)	1.278	1.250	1.228	1.298	2.118	0.195	24.5
Zw(Ti_L)	1.232	1.289	2.718	1.024	2.038	0.258	14.1

[a]At the ONIOM(M06L/6-311++G**:B3LYP/6-31G*)//ONIOM(B3LYP/6-31+G**:B3LYP/3-21G) level;
[b]Structures with canonical glycine are used for energy benchmarks;
[c]Interaction energies between glycine and zeolite in these cases.

of silanol (Si-OH) and titanol (Ti-OH) will spontaneously transform to canonical conformers, consistent with the results of one silanol defect on the silica surface[37]. In absence of zeolite channels, framework Al and Ga Lewis acidic sites alone can stabilize glycine in the zwitterionic form, while the canonical structures become more energetically preferential. As to defect titanol (Ti-OH), Ti Lewis acidic site alone fails to stabilize glycine in the zwitterionic form (supplementary Figure S5), while the synergetic action of H-bonding interactions from lattice-O atoms (supplementary Figure S4c) enables the zwitterionic glycine to represent as a stationary point. Thus, the comparisons of 6-T and 32-T calculated results clearly demonstrate that zeolite channels play an essential role during zwitterionic stabilization and significantly enhance the relative stability of zwitterionic vs. canonical structures.

Computational Methodologies

The three-coordinated framework Al and Ga sites in zeolites were constructed by removing the Si neighbour associated with the bridging hydroxyl of the Brönsted acidic sites (≡M-OH-Si≡)[13,17], see Figure 1. Analogously, the silanol/titanol defects were resulted by removal of one Si neighbour[36–38,48]. The local structures of zeolites for these defects were each represented by 32-T cluster models, and one of the Si12 atoms was replaced in the cases of heteroatom substitution (M = Al, Ga, Ti). The terminal Si and O atoms of the 32-T cluster models were saturated by H atoms, which were oriented towards what would be next lattice O and Si atoms in the crystallographic structure. The Si-H and O-H distances were then adjusted to 1.500 and 1.000 Å, respectively.

All calculations were performed with use of Gaussian09 software of packages[53], and the computational methods are in line with our previous works[17,42,54]. In the two-layer ONIOM scheme[55], the $(H_3SiO)_2M(OSiH_3)$ (M = Al, Ga) or $(H_3SiO)_2MOH(OSiH_3)$ (M = Si, Ti) portions of zeolites as well as adsorbents were selected as the high-level region and allowed to relax fully, while the rest (low-level region) were fixed during geometry optimizations. The B3LYP/6-31+G(d,p) and B3LYP/3-21G methods were used for the high-level and low-level regions, respectively. Assignment of transition state (TS) to a particular intramolecular proton transfer reaction was verified by perturbing the structure along the reaction path eigenvector in both directions following with geometry optimizations. On basis of optimized structures, the adsorption energies as well as reaction barriers and energies were computed by the two-layer ONIOM(M06L/6-311++G(d,p):B3LYP/6-31G(d)) methodology. M06L[56,57] is a meta-GGA (Generalized Gradient Approximation) functional that includes dispersive interactions, which may be significant for the adsorption and chemical reactions within zeolitic materials. As elaborated in the supplementary information, the above computational methods have been validated by a series of calculations using different functionals and basis sets[58–61].

To facilitate the understanding of the role of zeolite channels played during the zwitterionic stabilization, 6-T cluster models were also used, and more computational details can be found in the supplementary information.

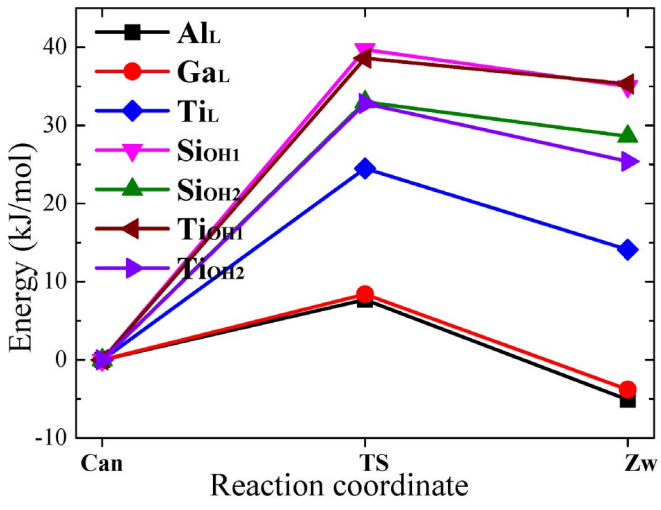

Figure 7 | Energy diagrams of the intramolecular proton transfer reactions between canonical (Can) and zwitterionic (Zw) glycine conformers adsorbed over framework M Lewis sites (M_L, M = Al, Ga, Ti) as well as defect hydroxyls of silanol and titanol. The local structures of MFI zeolite are represented by 32-T cluster models, and the two reaction paths of hydroxyl defects are differed by subscripts OH1 and OH2, corresponding to structures **Can1** (**Zw1**) and **Can2** (**Zw2**), respectively.

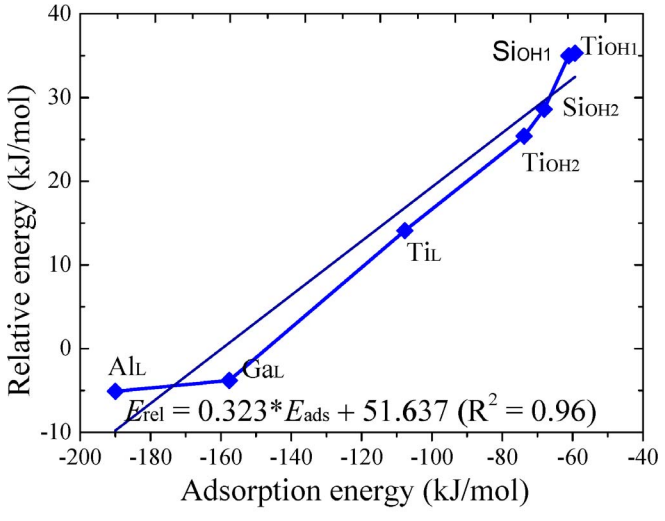

Figure 8 | Correlation between the relative stabilities of zwitterionic vs. canonical glycine and the adsorption energies of canonical glycine over framework M Lewis sites (M_L, M = Al, Ga, Ti) as well as defect hydroxyls of silanol and titanol. The local structures of MFI zeolite are represented by 32-T cluster models, and the two reaction paths of hydroxyl defects are differed by subscripts OH1 and OH2, corresponding to structures **Can1** (**Zw1**) and **Can2** (**Zw2**), respectively.

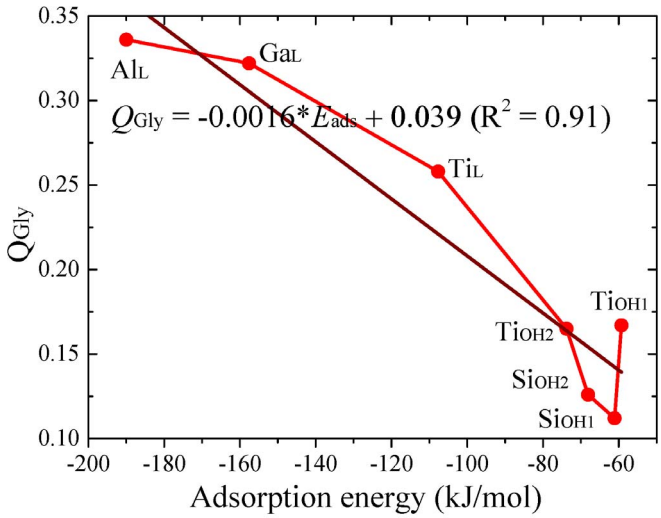

Figure 9 | Correlation between the net charges on zwitterionic glycine and the adsorption energies of canonical glycine over framework M Lewis sites (M_L, M = Al, Ga, Ti) as well as defect hydroxyls of silanol and titanol. The local structures of MFI zeolite are represented by 32-T cluster models, and the two reaction paths of hydroxyl defects are differed by subscripts OH1 and OH2, corresponding to structures **Can1** (**Zw1**) and **Can2** (**Zw2**), respectively.

1. Nagy, J. B. *et al. Isomorphs substitution in zeolites*, in: Karge, H. G. & Weitkamp, J. (Eds.), Molecular sieves (Vol. 5), Springer Berlin/Heidelberg, pp. 365–478 (2007).
2. Tuan, W. A., Falconer, J. L. & Noble, R. D. Isomorphous substitution of Al, Fe, B, and Ge into MFI-zeolite membranes. *Micropor. Mesopor. Mater.* **141**, 269–280 (2000).
3. Ratnasamy, P., Srinivas, D. & Knozinger, H. Active sites and reactive intermediates in titanium silicate molecular sieves. *Adv. Catal.* **48**, 1–169 (2004).
4. Liu, S. B. *et al.* On the thermal stability of zeolite beta. *J. Catal.* **132**, 432–439 (1991).
5. Zicovich-Wilson, C. M. & Dovesi, R. Titanium-containing zeolites. A periodic ab Initio Hartree-Fock characterization. *J. Phys. Chem. B* **102**, 1411–1417 (1998).
6. Yang, G. *et al.* On configuration of exchanged La^{3+} on ZSM-5: A theoretical approach to the improvement in hydrothermal stability of La-modified ZSM-5 zeolite. *J. Chem. Phys.* **119**, 9765–9770 (2003).
7. Xue, N. H. *et al.* Understanding the enhancement of catalytic performance for olefin cracking: Hydrothermally stable acids in P/HZSM-5. *J. Catal.* **248**, 20–28 (2007).
8. Bortnovsky, O., Sobafik, Z., Wichterlová, B. & Bastl, Z. Structure of Al-Lewis site in beta zeolite active in the Meerwein-Ponndorf-Verley reduction of ketone to alcohol. *J. Catal.* **210**, 171–182 (2002).
9. Boronat, M. *et al.* Determination of the catalytically active oxidation Lewis acid sites in Sn-beta zeolites, and their optimisation by the combination of theoretical and experimental studies. *J. Catal.* **234**, 111–118 (2005).
10. Román-Leshkov, Y., Moliner, M., Labinger, J. A. & Davis, M. E. Mechanism of Glucose Isomerization Using a Solid Lewis Acid Catalyst in Water. *Angew. Chem. Int. Ed.* **49**, 8954–8957 (2010).
11. Yang, G., Pidko, E. A. & Hensen, E. J. M. The mechanism of glucose isomerization to fructose over Sn-BEA zeolite: A periodic density functional theory study. *ChemSusChem* **6**, 1688–1696 (2013).
12. Janiszewska, E. *et al.* The role of the defect groups on the Silicalite-1 zeolite catalytic behavior. *Micropor. Mesopor. Mater.* **182**, 220–228 (2013).
13. van Bokhoven, J. A., van der Eerden, A. M. J. & Koningsberger, D. K. Three-Coordinate Aluminum in Zeolites Observed with In situ X-ray Absorption Near-Edge Spectroscopy at the Al K-Edge: Flexibility of Aluminum Coordinations in Zeolites. *J. Am. Chem. Soc.* **125**, 7435–7442 (2003).
14. Busco, C., Bolis, V. & Ugliengo, P. Masked Lewis Sites in Proton-Exchanged Zeolites: A Computational and Microcalorimetric Investigation. *J. Phys. Chem. C* **111**, 5561–5567 (2007).
15. Chang, Y. F., McCarty, J. G. & Zhang, Y. L. N_2O decomposition over [Fe]-ZSM-5 and Fe-HZSM-5 zeolites. *Catal. Lett.* **34**, 163–177 (1995).
16. Yuranov, I., Bulushev, D. A., Renken, A. & Kiwi-Minsker, L. Benzene hydroxylation over FeZSM-5 catalysts: which Fe sites are active? *J. Catal.* **227**, 138–147 (2004).
17. Yang, G. & Zhou, L. J. A DFT study on direct benzene hydroxylation catalyzed by framework Fe and Al sites in zeolites. *Catal. Sci. Technol.* **4**, DOI: 10.1039/C4CY00369A (2014).
18. Yu, D., Rauk, A. & Armstrong, D. A. Radicals and ions of glycine: An ab initio study of the structures and gas-phase thermochemistry. *J. Am. Chem. Soc.* **117**, 1789–1796 (1995).
19. Bouchoux, G. Gas phase basicities of polyfunctional molecules. Part 3: Amino acids. *Mass Spectrom. Rev.* **31**, 391–435 (2012).
20. Jensen, J. H. & Gordon, M. S. On the number of water molecules necessary to stabilize the glycine zwitterion. *J. Am. Chem. Soc.* **117**, 8159–8170 (1995).
21. Yamabe, S., Ono, N. & Tsuchida, N. Molecular interactions between glycine and H_2O affording the zwitterion. *J. Phys. Chem. A* **107**, 7915–7922 (2003).
22. Chowdhry, B. Z., Dines, T. J., Jabeen, S. & Withnall, R. Vibrational spectra of alpha-amino acids in the zwitterionic state in aqueous solution and the solid state: DFT calculations and the influence of hydrogen bonding. *J. Phys. Chem. A* **112**, 10333–10347 (2008).
23. Hwang, T. K. *et al.* Microsolvation of lysine by water: computational study of stabilized zwitterion. *J. Phys. Chem. B* **115**, 10147–10153 (2011).
24. Hoyau, S. & Ohanessian, G. Interaction of Alkali Metal Cations (Li^+-Cs^+) with Glycine in the Gas Phase: A Theoretical Study. *Chem. Eur. J.* **4**, 1561–1569 (1998).
25. Ai, H. Q., Bu, Y. X. & Han, K. L. Dipole bound and valence state coupling in argon-solvated nitromethane anions. *J. Chem. Phys.* **118**, no. 10973 (2003).
26. Constantino, E. *et al.* Interaction of Co^+ and Co^{2+} with glycine. A theoretical study. *J. Phys. Chem. A* **109**, 224–230 (2005).
27. Remko, M. & Rode, B. M. Effect of metal ions (Li^+, Na^+, K^+, Mg^{2+}, Ca^{2+}, Ni^{2+}, Cu^{2+}, and Zn^{2+}) and water coordination on the structure of glycine and zwitterionic glycine. *J. Phys. Chem. A* **110**, 1960–1967 (2006).
28. Yang, G. *et al.* Assembly and stabilization of multi-amino acid zwitterions by the Zn(II) Ion: A computational exploration. *J. Phys. Chem. B* **113**, 4899–4906 (2009).
29. Gutowski, M., Skurski, P. & Simons, J. Dipole-bound anions of glycine based on the zwitterion and neutral structures. *J. Am. Chem. Soc.* **122**, 10159–10162 (2000).
30. Xu, S. J., Zheng, W. J., Radisic, D. & Bowern, K. H., Jr. The stabilization of arginine's zwitterion by dipole-binding of an excess electron. *J. Chem. Phys.* **122**, no. 091103 (2005).
31. Kass, S. R. Zwitterion-dianion complexes and anion-anion clusters with negative dissociation energies. *J. Am. Chem. Soc.* **127**, 13098–13099 (2005).
32. Yang, G. *et al.* Stabilization of amino acid zwitterions with varieties of anionic species: The intrinsic mechanism. *J. Phys. Chem. B* **112**, 7104–7110 (2008).
33. Tian, S. X., Li, H. B. & Yang, J. L. Monoanion BH_4^- can stabilize zwitterionic glycine with dihydrogen bonds. *ChemPhysChem* **10**, 1435–1437 (2009).
34. Schmidt, J. & Kass, S. R. Zwitterion vs neutral structures of amino acids stabilized by a negatively charged site: Infrared photodissociation and computations of proline-chloride anion. *J. Phys. Chem. A* **117**, 4863–4869 (2013).
35. Derouane, E. G. Zeolites as solid solvents. *J. Mol. Catal. A: Chemical* **134**, 29–45 (1998).
36. Zheng, A. M. *et al.* Enhancement of Brønsted acidity in zeolitic catalysts due to an intermolecular solvent effect in confined micropores. *Chem. Commun.* **48**, 6936–6938 (2012).
37. Rimola, A. *et al.* Interaction of glycine with isolated hydroxyl groups at the silica surface: First principles B3LYP periodic simulation. *Langmuir* **22**, 6593–6604 (2006).
38. Rimola, A., Civalleri, B. & Ugliengo, P. Neutral vs zwitterionic glycine forms at the water/silica interface: structure, energies, and vibrational features from B3LYP periodic simulations. *Langmuir* **24**, 14027–14034 (2008).
39. Boekfa, B., Pantu, P. & Limtrakul, J. Interactions of amino acids with H-ZSM-5 zeolite: An embedded ONIOM study. *J. Mol. Struct.* **889**, 81–89 (2008).
40. Costa, D. *et al.* DFT study of the adsorption of microsolvated glycine on a hydrophilic amorphous silica surface. *Phys. Chem. Chem. Phys.* **10**, 6360–6368 (2008).
41. Rimola, A., Sodupe, M. & Ugliengo, P. Affinity scale for the interaction of amino acids with silica surfaces. *J. Phys. Chem. C* **113**, 5741–5750 (2009).
42. Yang, G., Zhou, L. J. & Liu, C. B. Glycine canonical and zwitterionic isomers within zeolites. *J. Phys. Chem. B* **113**, 10399–10402 (2009).
43. Rimola, A., Civalleri, B. & Ugliengo, P. Physisorption of aromatic organic contaminants at the surface of hydrophobic/hydrophilic silica geosorbents: a B3LYP-D modeling study. *Phys. Chem. Chem. Phys.* **12**, 6357–6366 (2010).
44. Zhao, Y. L., Koppen, S. & Frauenheim, T. An SCC-DFTB/MD study of the adsorption of zwitterionic glycine on a geminal hydroxylated silica surface in an explicit water environment. *J. Phys. Chem. C* **115**, 9615–9621 (2011).
45. Bouchoucha, M. *et al.* Glutamic acid adsorption and transformations on silica. *J. Phys. Chem. C* **115**, 21813–21825 (2011).
46. Stuckenschneider, K. *et al.* Amino-acid adsorption in MFI-Type zeolites enabled by the pH-dependent ability to displace water. *J. Phys. Chem. C* **117**, 18927–18935 (2013).
47. Stuckenschneider, K., Merz, J. & Schembecker, G. Molecular interaction of amino acids with acidic zeolite BEA: The effect of water. *J. Phys. Chem. C* **118**, 5810–5819 (2014).
48. Yang, G. *et al.* A joint experimental-theoretical study on trimethylphosphine adsorption on the Lewis acidic sites present in TS-1 zeolite. *J. Mol. Struct.* **882**, 24–29 (2008).
49. Fricke, R., Kosslick, H. & Lischke, G. Incorporation of gallium into zeolites: Syntheses, properties and catalytic application. *Chem. Rev.* **100**, 2303–2406 (2000).

50. Rimola, A. *et al.* Silica surface features and their role in the adsorption of biomolecules: Computational modeling and experiments. *Chem. Rev.* **113**, 4216–4313 (2013).
51. Damin, A., Bordiga, S., Zecchina, A. & Lamberti, C. Reactivity of Ti(IV) sites in Ti-zeolites: An embedded cluster approach. *J. Chem. Phys.* **117**, 226–237 (2002).
52. Shetty, S. *et al.* A comparative study of structural, acidic and hydrophilic properties of Sn-BEA with Ti-BEA using periodic density functional theory. *J. Phys. Chem. B* **112**, 2573–2579 (2008).
53. Gaussian 09, Revision D.01, Frisch, M. J. *et al.* Gaussian, Inc., Wallingford CT (2013).
54. Yang, Z. W., Yang, G., Liu, X. C. & Han, X. W. The direct hydroxylation of benzene to phenol catalyzed by Fe-ZSM-5 zeolite: A DFT and hybrid MP2:DFT calculation. *Catal. Lett.* **143**, 260–266 (2013).
55. Vreven, T. *et al.* Combining Quantum Mechanics Methods with Molecular Mechanics Methods in ONIOM. *J. Chem. Theory Comput.* **2**, 815–826 (2006).
56. Zhao, Y. & Truhlar, D. G. A new local density functional for main-group thermochemistry, transition metal bonding, thermochemical kinetics, and noncovalent interactions. *J. Chem. Phys.* **125**, no. 194101 (2006).
57. Zhao, Y. & Truhlar, D. G. The M06 suite of density functionals for main group thermochemistry, thermochemical kinetics, noncovalent interactions, excited states, and transition elements: two new functionals and systematic testing of four M06-class functionals and 12 other functionals. *Theor. Chem. Acc.* **120**, 215–241 (2008).
58. Schaefer, A., Horn, H. & Ahlrichs, R. Fully optimized contracted Gaussian-basis sets for atoms Li to Kr. *J. Chem. Phys.* **97**, 2571–2577 (1992).
59. Schaefer, A., Huber, C. & Ahlrichs, R. Fully optimized contracted Gaussian-basis sets of triple zeta valence quality for atoms Li to Kr. *J. Chem. Phys.* **100**, 5829–5835 (1994).
60. de Moor, B. A., Reyniers, M. F., Sierka, M. & Sauer, J. Physisorption and chemisorption of hydrocarbons in H-FAU using QM-Pot(MP2//B3LYP) calculations. *J. Phys. Chem. C* **112**, 11796–11812 (2008).
61. Svelle, S., Tuma, C., Rozanska, X., Kerber, T. & Sauer, J. Quantum chemical modeling of zeolite-catalyzed methylation reactions: Towards chemical accuracy. *J. Am. Chem. Soc.* **131**, 816–825 (2009).

Acknowledgments

We gratefully acknowledged the financial supports from the National Natural Science Foundation (No. 21473137) and Fundamental Research Funds for the Central Colleges (SWU113049, XDJK2014C106 and 2362014xk01). We thank National Supercomputing Center in Shenzhen for providing the computational resources and Gaussian09 software.

Author contributions

G.Y. designed the experiments and prepared the manuscript. L.J.Z. helped analyze the results. All authors reviewed and approved the manuscript.

Additional information

Supplementary information accompanies this paper at http://www.nature.com/scientificreports

Competing financial interests: The authors declare no competing financial interests.

How to cite this article: Yang, G. & Zhou, L. Zwitterionic versus canonical amino acids over the various defects in zeolites: A two-layer ONIOM calculation. *Sci. Rep.* **4**, 6594; DOI:10.1038/srep06594 (2014).